

Mössbauer spectroscopic studies of $\text{Nd}_2\text{Fe}_{14}\text{B}$

R. Kamal

Department of Physics, Punjabi University, Patiala 147002, Punjab, India

Y. Andersson

Institute of Chemistry, Uppsala University, S-751 21 Uppsala, Sweden

(Received 3 August 1984; revised manuscript received 7 March 1985)

$\text{Nd}_2\text{Fe}_{14}\text{B}$ has been synthesized from the constituent elements by arc melting and annealing at 1400 K. [The tetragonal-unit-cell dimensions were determined to be $a=8.8045(3)$ Å; $c=12.2031(5)$ Å]. ^{57}Fe Mössbauer spectra have been recorded in the temperature range 80–640 K. The Curie temperature was found to be 581(1) K. With the use of the available crystal-structure information, the spectra have been analyzed in terms of six crystallographically nonequivalent iron sites. For each of these sites, the magnetic hyperfine field, the isomer shift, the quadrupole splitting, and the variation of these parameters with temperature were determined.

INTRODUCTION

Croat and co-workers^{1–3} discovered magnetic hardening in melt-spun Nd-Fe-B ribbons which also exhibited very high energy products. Therefore, there is at present some considerable interest^{4,5} in the study of Nd-Fe-B intermetallic compounds. Sagawa *et al.*⁶ have reported that such a compound, $\text{Nd}_{12}\text{Fe}_{82}\text{B}_6$, can be prepared by powder metallurgy where both the Nd and Fe atoms exhibit the desired uniaxial anisotropies in the magnetic material. Single-crystal-structure determinations by Givord *et al.*⁷ and Shoemaker *et al.*⁸ and neutron powder diffraction studies by Herbst *et al.*⁹ have shown that the ideal composition corresponds to the formula $\text{Nd}_2\text{Fe}_{14}\text{B}$. $\text{Nd}_2\text{Fe}_{14}\text{B}$ crystallizes in space group $P4_2/mnm$ (D_{4h}^{14}). Each unit cell contains eight neodymium atoms situated on two fourfold positions on 4*f* and 4*g* and 56 iron atoms situated on two fourfold positions on 4*c* and 4*e*, two eightfold positions on 8*j* and two sixteenfold positions on 16*k*, and four boron atoms on one fourfold position on 4*f*.

Mössbauer studies^{10–15} have been made in the past on a number of rare-earth iron alloys $R_x\text{Fe}_y$. In the present paper the results of a Mössbauer spectroscopy study of $\text{Nd}_2\text{Fe}_{14}\text{B}$ in the temperature range 80–640 K are reported. The spectra have been analyzed on the basis of the crystal structure.

EXPERIMENTAL DETAILS

Preparation and x-ray diffraction work

Appropriate amounts of the elements neodymium (99.99% purity, Rare Earths Products Ltd.) and iron (rod, 99.995% purity, Highways) and boron (chips, claimed purity 99.8%, Koch-Light Laboratories, Ltd.) were melted twice in an arc furnace in an argon atmosphere. This product was heat-treated at 1400 K for six hours in a water-cooled copper crucible in an induction furnace filled with argon.

X-ray powder diffraction patterns were recorded in a

focusing Hägg-Guinier-type camera using Cr K_{α_1} radiation and silicon as internal calibration standard ($a=5.430739$ Å). The unit-cell parameters were refined with the least-squares method to $a=8.8045(3)$ Å and $c=12.2031(5)$ Å. In addition to the lines belonging to the $\text{Nd}_2\text{Fe}_{14}\text{B}$ phase there were a few lines too weak for identification.

Mössbauer spectroscopy

The alloy was crushed to a fine powder and mixed with boron nitride. The mixture was pressed to a disk containing 34 mg/cm² of natural iron. Mössbauer spectra were recorded in an absorber mode using a microcomputer-controlled constant acceleration drive^{16,17} with two $^{57}\text{CoRh}$ sources permitting simultaneous calibration using a natural iron foil at room temperature as standard. The temperature of the sample was varied using an Oxford Instrument Cryostat (80–300 K) and a vacuum furnace (300–640 K). The recorded spectra were folded and analyzed using an interacting computer program¹⁸ featuring as few approximations as possible when treating the physical problems involved and capable of solving the combined interaction Hamiltonian. This program calculated the transmission integral for the given absorber thickness (effective absorber thickness $t_a \approx 5$ in the present case). A direct connection between the Digital Equipment Corporation VAX-11/750 computer and the Mössbauer data collection system was used to transfer the data before running this program.

The constraints associated with the computer fit of the spectra were as follows: (a) Six subspectra were assumed in intensity ratios 4:4:2:2:1:1. To a subspectrum within a set of two subspectra of equal intensity, the assignment to a particular nonequivalent iron position (site) within a unit cell was made on the basis of the number of near neighbors (NN) ferromagnetically coupled at that site. Therefore, the site where $n_{\text{NN}}(\text{Fe}) + n_{\text{NN}}(\text{Nd})$ was greater was assumed to have a higher internal hyperfine field, B_{hf} . (b) As the intensity ratio was constrained to

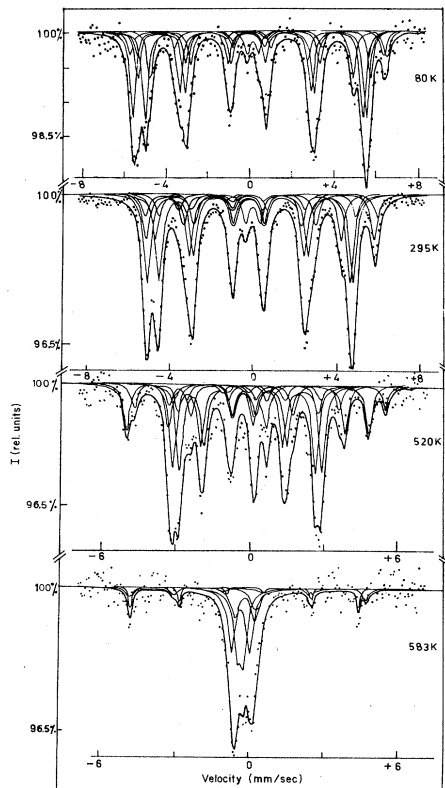


FIG. 1. Mössbauer spectra at $T = 80, 295, 520,$ and 583 K in $\text{Nd}_2\text{Fe}_{14}\text{B}$. The results of computer fitting with (i) relative intensities constrained in ratios of site occupancies within the unit cell, and (ii) line shape and linewidth constrained to one given by complete transmission integral for $t_a = 5$. Spectra at intermediate T values not shown. The background counts are around one million.

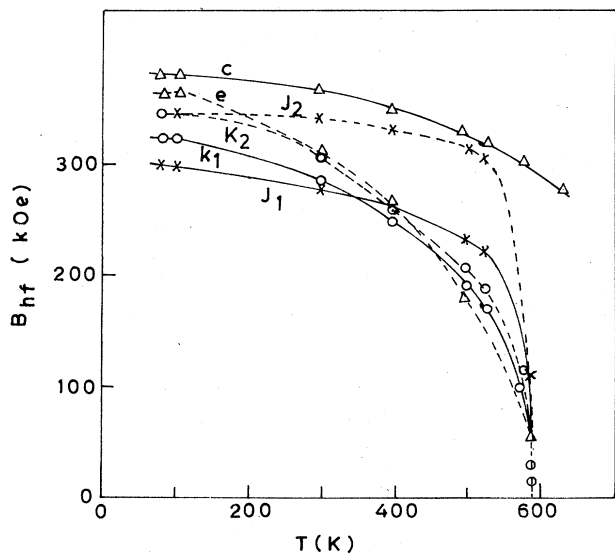


FIG. 2. Hyperfine internal magnetic field B_{hf} at six different nonequivalent magnetic sites as a function of T . T dependence for different sites is shown by a solid line for $k_1, j_1,$ and c sites and a dashed line for $k_2, j_2,$ and e sites. The experimental computed values for different sites are shown as \circ — k sites, \times — j sites, and Δ — e and c sites.

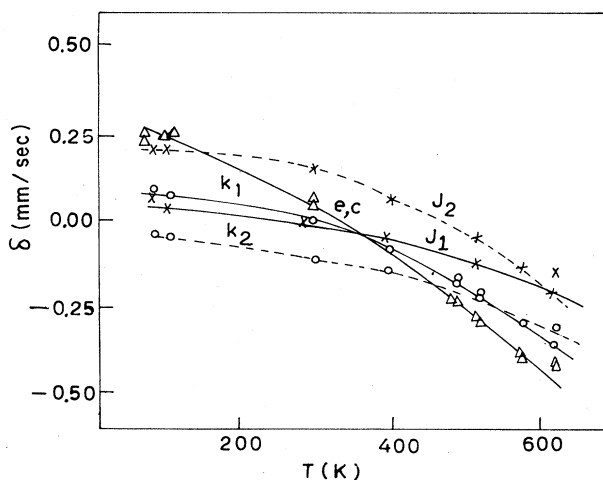


FIG. 3. Isomer shift δ with respect to Fe metal foil of $t_a = 7.5$ used simultaneously for calibration during recording of the spectra. T dependence for different sites shown by a solid line for $k_1, j_1,$ and c sites and a dashed line for $k_2, j_2,$ and e sites. The computed values from experimental data for different sites are shown as \circ — k sites, \times — j sites and Δ — e and c sites.

4:2:1 in each set at all temperatures T , the T dependence of the recoilless fractions of Fe atoms at the different sites was thus assumed to be the same. (c) Linewidths of the six subspectra were also taken to be the same. (d) Line shape was assumed to be as expected from the transmission integral for the given absorber thickness. (e) Electric-field gradients q were taken as axially symmetric

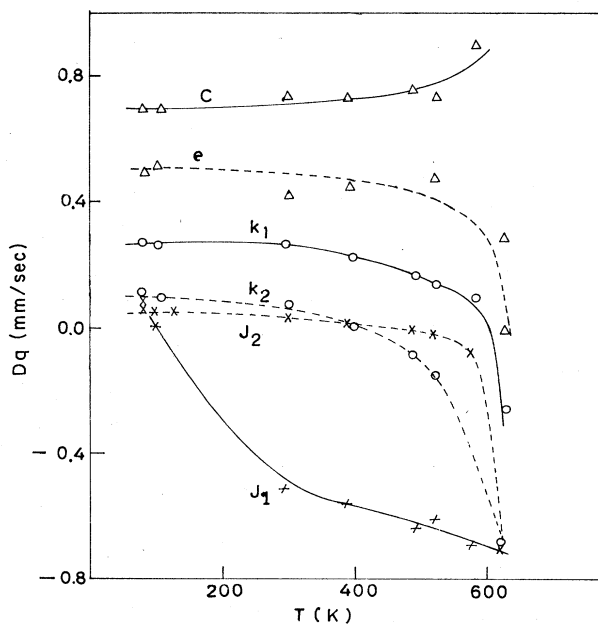


FIG. 4. Quadrupole splitting $Dq = \left| \frac{1}{4} e^2 q Q (3 \cos^2 \theta - 1) \right|$ assuming the axial field symmetry of electric-field gradient present along with the internal magnetic field. T dependence for different sites is shown by a solid line for $k_1, j_1,$ and c sites and by a dashed line for $k_2, j_2,$ and e sites. The compound values from experimental data are shown as \circ — k sites, \times — j sites, and Δ — e and c sites.

at all Fe sites, as the crystal structure is uniaxially anisotropic. This meant that the quadrupole splitting $Dq = \frac{1}{4}e^2qQ(3\cos^2\theta - 1)$ where Q is the nuclear quadrupole moment and θ is the angle between the direction of magnetization and the axially symmetric electric-field gradient which is along the axis of local symmetry. (f) The spin texture parameter,¹⁹ the measure of deviation from the usual intensity ratios 3:2:1:1:2:3 of the Zeeman lines in each subspectra, was also assumed to be the same at all six sites.

Figure 1 shows the select Mössbauer spectra between 80 and 640 K. Figures 2, 3, and 4 show the T dependences of estimated parameters B_{hf} , δ , and Dq for each of the six sites.

RESULTS AND DISCUSSION

The crystal structure of $\text{Nd}_2\text{Fe}_{14}\text{B}$ can be described as a stacking of three different types of layers. Two of these layers consist of iron atoms which form nets of distorted hexagons and triangles. These layers are interconnected in pairs by iron atoms, similar to the σ phase. The third layer contains neodymium, boron, and iron atoms in a triangular net. This layer and the connection to the σ -phase-type sequence is closely related to the CaCu_5 -type structure.

The unit-cell dimensions of the $\text{Nd}_2\text{Fe}_{14}\text{B}$ sample are in very good agreement with the values given by Shoemaker *et al.*⁸ [$a = 8.804(5)$ Å; $c = 12.205(5)$ Å], while somewhat different values are reported by Givord *et al.*⁷ ($a = 8.792$ Å; $c = 12.190$ Å) and Spada *et al.*²⁰ ($a = 8.792$ Å; $c = 12.174$ Å). While Givord *et al.*⁷ reported the composition of a tetragonal phase as $\text{Nd}_2\text{Fe}_{14}\text{B}$, Spada *et al.*²⁰ reported the composition as $\text{Nd}_3\text{Fe}_{20}\text{B}_2$ even though their a and c values were surprisingly matching. The difference between our results and those of Givord *et al.*⁷ could be due to a range of homogeneity, but so far no investigation on this subject has been reported.

Average internal hyperfine field \bar{B}_{hf}

Assuming the statistical distribution of Fe atoms at the nearest-neighbor positions in a $R_x\text{Fe}_y$ alloy, one can estimate¹⁴ the average magnetic moments $\bar{\mu}$. For the $\text{Nd}_2\text{Fe}_{14}$ alloy, the μ is estimated as $2.1\mu_B$. Assuming a ratio of $145 \text{ kOe}/\mu_B$ between B_{hf} and μ ,²¹ \bar{B}_{hf} is estimated as 304 kOe. \bar{B}_{hf} at 295 K from Fig. 2 is 302 kOe. Therefore, there is close agreement at higher T only. At lower T \bar{B}_{hf} is higher than this value and in fact $\bar{B}_{\text{hf}}(80 \text{ K}) = 337$ kOe (Fig. 2) and $\bar{B}_{\text{hf}}(T \rightarrow 0 \text{ K}) = 347$ kOe. A recent Mössbauer study²² in melt-spun Nd-Fe-B ribbon containing $\text{Nd}_2\text{Fe}_{14}\text{B}$ also shows $\bar{B}_{\text{hf}}(300 \text{ K}) = 300$ kOe, which is in close agreement to the present result at room temperature.

Gubbens *et al.*¹¹ had observed nearly a linear relationship between the $B_{\text{hf}}(4 \text{ K})$ in $R_x\text{Fe}_y$ alloys of different crystal structures and the relative number of near iron neighbors $n_{\text{NN}}(\text{Fe})/[n_{\text{NN}}(\text{Fe}) + n_{\text{NN}}(\text{R})]$. Using their graph¹¹ for B_{hf} at 4.2 K, in the $\text{Nd}_2\text{Fe}_{14}$ alloy, \bar{B}_{hf} is estimated as 331 kOe. Therefore, it appears that the present results show higher \bar{B}_{hf} than those from the above theoretical predictions. These predictions are based upon

the fact that usually the $4f$ interactions do not induce the additional $3d$ moments significantly thereby resulting in the observation of linear relationships¹¹ with the iron coordination.

A polarized neutron study recently communicated to us by Givord and Li²³ shows that $\bar{\mu} = 2.57\mu_B$ for iron moments considering a $3d$ contribution alone and $\bar{\mu} = 2.37\mu_B$ considering $3d$ and $4s$ contributions together in $\text{Nd}_2\text{Fe}_{14}\text{B}$ at 4.2 K. The estimated \bar{B}_{hf} for the Mössbauer measurements is thus 344 kOe using a $145 \text{ kOe}/\mu_B$ value.²¹ Our low- T values therefore are in very close agreement with the polarized neutron data.²³ There is also a very close agreement with a recent spontaneous magnetization study.²⁴ It appears that in $\text{Nd}_2\text{Fe}_{14}\text{B}$, the $4f$ interactions induce to a significant extent the additional $3d$ moments, which causes a greater core polarization and therefore a higher \bar{B}_{hf} than usual in $R_x\text{Fe}_y$ alloys.¹⁰⁻¹⁵

B_{hf} at six magnetically nonequivalent sites

One of the advantages of ^{57}Fe Mössbauer spectroscopy is that like polarized neutron studies, it allows one to distinguish between B_{hf} values of Fe atoms belonging to the different crystallographic sites. For the Fe atom situated on two different $16k$ positions, at the k_1 site $n_{\text{NN}}(\text{Fe}) = 9$, $n_{\text{NN}}(\text{B}) = 1$, $n_{\text{NN}}(\text{Nd}) = 2$; and at the k_2 site $n_{\text{NN}}(\text{Fe}) = 10$, $n_{\text{NN}}(\text{Nd}) = 2$. The $\bar{d}_{\text{Fe-Fe}}(k_1)$ and $\bar{d}_{\text{Fe-Fe}}(k_2) = 2.584$ and 2.535 Å, respectively. As the number of Nd neighbors is the same, the effects of induced $3d$ moments due to $4f$ interactions are the same, so the difference in B_{hf} at $T \rightarrow 0$ can be ascribed to the change in $n_{\text{NN}}(\text{Fe})$. $B_{\text{hf}}(k_2)$ is expected to be greater than $B_{\text{hf}}(k_1)$ due to a higher Fe coordination as well as a lower $\bar{d}_{\text{Fe-Fe}}$. The difference of 23 kOe (Fig. 2) is equal to the value expected from the linear relationship.¹¹ Therefore, both the differences in B_{hf} as well as the fact that $B_{\text{hf}}(k_2) > B_{\text{hf}}(k_1)$ can be explained physically from the core polarization effects alone.

For the two $8j$ positions, at the j_1 site, $n_{\text{NN}}(\text{Fe}) = 9$, $n_{\text{NN}}(\text{Nd}) = 3$; and the j_2 site, $n_{\text{NN}}(\text{Fe}) = 12$, $n_{\text{NN}}(\text{Nd}) = 2$. Neglecting the $3d$ - $4f$ interactions, the linear relationship predicts $B_{\text{hf}}(j_2) > B_{\text{hf}}(j_1)$ and the difference in B_{hf} as 34 kOe. The $3d$ - $4f$ interactions are due to the higher value of $n_{\text{NN}}(\text{Nd})$ at the j_1 site, which is expected to decrease. However, the experimentally observed difference is 44 kOe (Fig. 2). The deviation could be explained as due to (1) the decrease of magnetic interactions at very short $d_{\text{Fe-Fe}}$ when $d < 2.4$ Å ($d_{\text{Fe-Fe}}$ varies over a wide range, 2.396 and 2.784 Å at the j_1 site, with two of the Fe atoms at 2.396 Å), and (2) the different contributions to the transferred hyperfine fields because of conduction-electron polarization by the surrounding moments when there is a wide difference in $\bar{d}_{\text{Fe-Fe}}$ ($= 2.549$ and 2.698 Å at the j_1 and j_2 sites, respectively). The polarized neutron study²³ shows the first effect as definitely present at the j_1 site.

For the $4e$ and $4c$ positions at the e site, $n_{\text{NN}}(\text{Fe}) = 9$, $n_{\text{NN}}(\text{Nd}) = 2$, $n_{\text{NN}}(\text{B}) = 2$, and $\bar{d}_{\text{Fe-Fe}} = 2.589$ Å; and at the c site, $n_{\text{NN}}(\text{Fe}) = 8$, $n_{\text{NN}}(\text{Nd}) = 4$, and $\bar{d}_{\text{Fe-Fe}} = 2.532$ Å. While the linear relationship between B_{hf} and $n_{\text{NN}}(\text{Fe})$ predicts $B_{\text{hf}}(e) > B_{\text{hf}}(c)$, the considerations of a higher

number of ferromagnetically coupled neighbors $n_{\text{NN}}(\text{Fe}) + n_{\text{NN}}(\text{Nd})$, the expected μ enhancement by $3d-4f$ interactions, the presence of two boron atoms near the e site, and the interatomic distances with the neighbors suggest that $B_{\text{hf}}(c)$ should be greater than $B_{\text{hf}}(e)$. The polarized neutron study²³ has now demonstrated that (i) the $3d$ moment at the c site, $\mu(c)$, is in fact higher than the μ at the e site, (ii) $\mu(c)$ as well as $\mu(j_2)$ are in fact highest compared to μ at other sites in Nd₂Fe₁₄B, and (iii) in isostructural Y₂Fe₁₄B, the $\mu(c)$ is indeed the lowest. In Fe atoms, especially those surrounded by 4Nd neighbors, an additional contribution to the $3d$ moment is in fact found²³ to be significant, due to the polarization of the $3d$ band by $4f$ interactions in Nd₂Fe₁₄B. In Y₂Fe₁₄B, the additional contribution from $3d-4f$ coupling is absent.²³ The assignment in Fig. 2 appears correct and $B_{\text{hf}}(c) > B_{\text{hf}}(e)$.

We conclude from the above discussion that the correlation of B_{hf} to $n_{\text{NN}}(\text{Fe})$ expected from the linear relationship¹¹ is limited to the subspectra from the k_1 and k_2 sites. The effect of ferromagnetic coupling between Fe and Nd and the finite contribution of $4f$ interactions to $3d$ core polarization cannot be neglected. The effect of reduced magnetic interactions at a very short Fe-Fe distance is also noticeable in $B_{\text{hf}}(j_1)$.

From the polarized neutron study²³ the $3d$ moments are in the order $\mu(j_2) > \mu(c) > \mu(k_2) = \mu(k_1) > \mu(j_1) > \mu(e)$. Szpunar²⁵ is reported to have performed theoretical spin-polarized energy-band calculations which also suggests this order. In Fig. 2, the observation that at $T=300$ K the $B_{\text{hf}}(j_2)$ and $B_{\text{hf}}(k_1)$ are the highest, $B_{\text{hf}}(j_1)$ is least, and $B_{\text{hf}}(k_2)$ and $B_{\text{hf}}(k_1)$ lie in between is in agreement with these results.²³ However, the following discrepancy can be noticed: (i) $B_{\text{hf}}(T \rightarrow 0)$ at the e site is quite high, (ii) $B_{\text{hf}}(c) > B_{\text{hf}}(j_2)$ instead of $B_{\text{hf}}(j_2) > B_{\text{hf}}(c)$, and (iii) $B_{\text{hf}}(k_2) \neq B_{\text{hf}}(k_1)$ [we find that $B_{\text{hf}}(c) > B_{\text{hf}}(e) > B_{\text{hf}}(j_2) > B_{\text{hf}}(k_2) > B_{\text{hf}}(k_1) > B_{\text{hf}}(j_1)$]. One possibility is that in B_{hf} the contribution of the Fermi contact term due to delocalized $4s$ polarization is to be taken care of as well as the $3d$ core polarization effects. This contribution is neither observed in the polarized neutron study²³ nor is accounted for in theoretical calculations.²⁵ It is also likely that the computer fit is not unambiguous for the e and c sites because of the lowest population in the unit cell with respect to other sites. The direction of internal field at the nucleus has also been assumed to be the same at all the sites in our analysis.

Curie temperature and temperature dependence of B_{hf}

From Fig. 2, the Curie temperature, T_C is 581 ± 1 K. The T_C reported by Herbst *et al.*⁹ for Nd₂Fe₁₄B is 627 K, by Givord and Li²³ is 595 K, and by Sagawa *et al.*⁶ is 585 K (Nd₂Fe_{13.7}B). The measurement of T_C by Mössbauer spectroscopic measurement is truly the zero field T_C of the sample. This fact can explain the variance between the different results. The observed T_C is reduced to nearly half compared to T_C for α iron and this reduction is usually observed in $R_2\text{Fe}_{17}$ alloys²⁶ and is assigned to a significant decrease in $3d-3d$ exchange interactions between Fe-Fe neighbors. It is sometimes associated²⁶ with the occurrence of negative exchange interactions for short

Fe-Fe distances ($d_{\text{Fe-Fe}} < 2.4$ Å) following the Bethe-Slater and Néel arguments.²⁷ However, the validity of the Bethe-Slater curve is also doubtful.²⁸ But whether the negative exchange interactions between Fe-Fe neighbors occur or the significant reduction in $+ve$ exchange interaction occur, on both these accounts, one expects a greater T dependence of $3d$ magnetic moment and hence of B_{hf} for the site where shorter Fe-Fe distances occur and $d_{\text{Fe-Fe}}$ is smaller than for the sites where $d_{\text{Fe-Fe}}$ is larger (provided $d_{\text{Fe-Fe}}$ is not too large to significantly decrease exchange interaction). Using the $d_{\text{Fe-Fe}}$ values from the crystal-structure analysis at 300 K, one expects that σ is defined as $B_{\text{hf}}(T)/B_{\text{hf}}(T \rightarrow 0 \text{ K})$ in the order $\sigma(c) < \sigma(k_2) < \sigma(j_1) < \sigma(k_1) < \sigma(e) < \sigma(j_2)$ on the assumption that the $3d-3d$ exchange interaction alone is contributing to B_{hf} . The $\sigma(T)$ at $T=0.5T_C$ and $0.75T_C$ in Fig. 2 shows $\sigma(k_2) < \sigma(k_1) < \sigma(e) < \sigma(j_1) < \sigma(c) < \sigma(j_2)$. This result is not unexpected. The presence of a $3d-4f$ interaction causes the $3d$ shell deformation and increased core polarization at the c and j_1 sites as $n_{\text{NN}}(\text{Nd})=4$ and 3, respectively, while $n_{\text{NN}}(\text{Nd})=2$ at all other sites. This explains the higher values of $\sigma(c)$ and $\sigma(j_1)$ at a given T/T_C . The polarized neutron study of the T dependences of $3d$ moments is not available for Nd₂Fe₁₄B at present to enable us to compare the present results with other measurements.

Isomer shifts at six sites

The δ at a given site increases with the decrease in $4s$ electron density. The $4s$ electron density decreases with (i) the increase in the near-neighbor distances, of (ii) the increase in $3d$ core polarization causing a more effective shielding of the $4s$ electrons, and therefore, reducing the electron charge density. At 295 K,

$$\begin{aligned} \bar{d}_{\text{Fe-Fe}}(j_2) > \bar{d}_{\text{Fe-Fe}}(e) > \bar{d}_{\text{Fe-Fe}}(k_1) > \bar{d}_{\text{Fe-Fe}}(j_1) \\ > \bar{d}_{\text{Fe-Fe}}(k_2) > \bar{d}_{\text{Fe-Fe}}(c) . \end{aligned}$$

The δ values in Fig. 3 exhibit the relation $\delta(j_2) > \delta(e) > \delta(k_1) > \delta(j_1) > \delta(k_2)$ and $\delta(e) \approx \delta(c)$. The value of $\delta(c)$, higher than expected from the $\bar{d}_{\text{Fe-Fe}}$ value, can be explained due to very high $3d$ core polarization at the c site.²³

The T dependences at low T are usually related to effective Debye temperatures for each of the sites and the thermal expansion along the a and c axes. At high T , the δ depends on a second-order Doppler (SOD) shift which gives a linear decrease with T in the harmonic vibrational approximation. More detailed investigation is called for in order to explain the values of δ at different T in Fig. 3.

Quadrupole splittings at six sites

The average $[Dq]_{\text{av}}$ shows a sharp change at low T (Fig. 4) and a sharp change at T near T_C and this effect cannot be explained from the usual relation for q in alloys where $q(T) = A(1 - BT^{3/2})$. For the axially symmetric case $Dq = |\frac{1}{4}e^2qQ(3\cos^2\theta - 1)|$. Lately, a spontaneous magnetization study²⁴ has shown that below 135 K there is a change of the angle between the easy magnetization

direction and the c axis, and at 100 K this angle is 20° . $[Dq]_{av}$ (300 K) = 0.26 mm/sec, and $[Dq]_{av}$ (100 K) = 0.21 mm/sec (Fig. 4). This corresponds to the angular change of 21° . Hence, the sharp change in Dq at low T can be explained by the angular change θ . The sharp change near T_C as $T \rightarrow T_C$ can be explained by the anomalously large thermal expansion at low T , larger than at $T \rightarrow T_C$ in $R_2Fe_{14}B$.²⁸ Below T_C , the magnetically induced contributions²⁹ can also be present.

The largest change is noticed in $Dq(j_1)$ at low T . This could be due to the fact that the j_1 site has the two shortest Fe-Fe and has the largest deviations in d_{Fe-Fe} from \bar{d}_{Fe-Fe} , and the contribution to q is inversely related to the d_{Fe-Fe}^3 in the point-charge model.

The least T dependence of Dq at the j_2 site can be explained by the highest number of $n_{NN}(Fe)$ which are also arranged in σ -type coordination and the highest value of d_{Fe-Fe} . The smallest value of $Dq(j_2)$ is in accordance with symmetry at the j_2 site.

Spin-texture effects and anisotropy

Within $\pm 2\%$, the spin-texture parameter¹⁹ is unity at all six sites at all T values. The presence of a single hyperfine pattern for each nonequivalent site and the absence of the spin texture in the powdered specimen is expected from the absence of the basal-plane magnetic anisotropy usually noticed in R_2Fe_{17} alloys^{10,26} and the structural evidence⁷⁻⁹ of uniaxial magnetic anisotropy in $Nd_2Fe_{14}B$.

Central doublet

Most of the spectra (Fig. 1) fitted well with the assumption of six sites. However, a central doublet of fractional area between 3 to 5.5%, $Dq \approx 0.55$ mm/sec, $\delta(80\text{ K}) \approx 0.187$ mm/sec, and $\delta(T)$ varying as normal, effects expected from SOD could not be ruled out. This explained the unfitted central dip clearly noticeable in the low- T spectra (Fig. 1). The x-ray lines in addition to those belonging to the $Nd_2Fe_{14}B$ phase were so weak and diffused that they could not be said to belong to a new intermediate phase. Similar conclusions have been made by Shoemaker *et al.*⁸ in $Nd_2Fe_{14}B$ of cell dimensions very close to the samples of the present study. Their⁸ single-crystal refinements did not show any deviation from ideal stoichiometry. However, no one has done any reliable investigation into the range of homogeneity. The paramagnetic doublet could therefore arise when at a given site $n_{NN}(Fe) < 6$ due to statistical effects as in disordered R_xFe_y alloys.¹⁴

ACKNOWLEDGMENTS

Discussion with Docent Tore Ericsson and the help of Dr. Tore Sundqvist are acknowledged. One of us (R.K.) is grateful to the research leader of the nuclear hyperfine interaction Mössbauer Spectroscopy Group, Professor Roger Wäppling, for providing the opportunity to carry on the present work at Uppsala and to Dr. Lennart Hesselgren, Director, International Seminar in Physics, Uppsala University for arranging some financial support. Thanks are also expressed to Dr. Givord and co-workers for communicating to us the results of their latest measurements prior to publication.

- ¹J. J. Croat, IEEE Trans. Magn. 18, 1442 (1982).
²J. J. Croat, J. F. Herbst, R. W. Lee, and F. E. Pinkerton, Appl. Phys. Lett. 44, 148 (1984).
³J. J. Croat, J. F. Herbst, R. W. Lee, and F. E. Pinkerton, J. Appl. Phys. 55, 2078 (1984).
⁴D. J. Sellmyer, A. Ahmed, G. Muench, and G. Hadjipanayis, J. Appl. Phys. 55, 2088 (1984).
⁵J. J. Becker, J. Appl. Phys. 55, 2067 (1984).
⁶M. Sagawa, S. Fujimura, N. Togawa, H. Yamamoto, and Y. Matsuura, J. Appl. Phys. 55, 2083 (1984).
⁷D. Givord, H. S. Li, and J. M. Moreau, Solid State Commun. 50 497 (1984).
⁸C. B. Shoemaker, D. P. Shoemaker, and R. Fruchart, Acta Crystallogr. C 40, 1665 (1984). C. B. Shoemaker and D. P. Shoemaker, in Abstract No. 07.9-15, Proceedings of the International Conference of Crystallography, Hamburg (unpublished).
⁹J. F. Herbst, J. J. Croat, F. E. Pinkerton, and W. B. Yelon, Phys. Rev. B 29, 4176 (1984).
¹⁰P. C. M. Gubbens, J. J. Van Loef, and K. H. J. Buschow, J. Phys. (Paris) Colloq. C6-617 (1974).
¹¹P. C. M. Gubbens, A. M. van der Kraan, and K. H. J. Buschow, Solid State Commun. 26, 107 (1978).
¹²J. B. A. Elemans, P. C. M. Gubbens, and K. H. J. Buschow, J. Less Common Met. 44, 51 (1976).
¹³M. Shimotomai, H. Miyake, S. Komatsu, and M. Doyama, Hyperfine Interact. 11, 223 (1981).
¹⁴J. Chappert, R. Arrese-Boggiano, and J. M. D. Coey, in Proceedings of the International Conference on Magnetic Alloys & Oxides, Haifa (Israel), 1977 (unpublished).
¹⁵C. Meyer, F. Hartmann-Boutron, Y. Gros, and Y. Berthier, J. Phys. (Paris) 42, 605 (1981).
¹⁶T. Sundqvist and R. Wäppling, Nucl. Instrum. Methods 205, 473 (1983).
¹⁷T. Sundqvist (unpublished).
¹⁸P. Jernberg and T. Sundqvist, University of Uppsala Institute of Physics, Report No. UUIP-1090, 1983 (unpublished).
¹⁹T. Ericsson and R. Wäppling, J. Phys. C (Paris) Colloq. 37, C6-719 (1976).
²⁰F. Spada, C. Abache, and H. Oesterreicher, J. Less Common Met. 99, L21 (1984).
²¹P. C. M. Gubbens, J. H. F. van Apeldoorn, A. M. Vander Kraan, and K. H. J. Buschow, J. Phys. F 4, 921 (1974).
²²F. E. Pinkerton and W. R. Dunham, Bull. Am. Phys. Soc. 29, 322 (1984).
²³D. Givord and H. S. Li, J. Appl. Phys. (to be published).
²⁴D. Givord, H. S. Li, and R. P. Bathie, Solid State Commun. 51, 857 (1984).
²⁵B. Szpunar, J. Appl. Phys. (to be published).
²⁶D. Givord and R. Lemaire, IEEE Trans. Mag. MAG-10, 109

- (1974).
- ²⁷L. Néel, Ann. Phys. (N.Y.) 5, 232 (1936); C. Herring, in *Magnetism*, edited by G. T. Rado and H. Suhl (Academic, New York, 1966), Vol II.
- ²⁸D. Givord, H. S. Li, J. M. Moreau, and R. P. Bathie, Physica (Utrecht) (to be published).
- ²⁹U. Ganiel and S. Shtrikam, Phys. Rev. 167, 258 (1968); R. Kamal and R. G. Mendiratta, Phys. Rev. B 5, 1659 (1971).